18. T. E. F. Costa, H. Suh, M. C. Nussenzweig, *Proc. Natl. Acad. Sci. U.S.A.* **89**, 2205 (1992).
19. M. Reth, T. Imanishi-Kari, K. Rajewsky, *Eur. J. Immunol.* **9**, 1004 (1978).
20. A. Nussenzweig *et al.*, *Nature* **382**, 551 (1996); C. Zhu *et al.*, *Cell* **86**, 379 (1996).
21. R. Casellas *et al.*, in preparation.
22. It takes 36 hours for $\mu^{V+}\kappa^{V+}$ cells to enter the cell cycle, and only 15 to 20% of the cells are in the S or G_2 phase at 48 hours. After 48 hours 15 to 20% of the cells die, and there is no net increase in the total number of live B cells. Therefore, even if we assume a 6-hour cell cycle, selective expansion of small subpopulations of cells does not account for the loss of idiotype expression.
23. M. Hikida, M. Mori, T. Kabawata, T. Takai, H. Ohmori, *J. Immunol.* **158**, 2509 (1997).
24. M. Reth, P. Gehrmann, E. Petrac, P. Wiese, *Nature* **322**, 840 (1986); R. Kleinfield *et al.*, *ibid.*, p. 843; C. Chen, Z. Nagy, E. L. Prak, M. Weigert, *Immunity* **3**, 747 (1995).
25. F. W. Alt *et al.*, *EMBO J.* **3**, 1209 (1984).
26. J. Foote and C. Milstein, *Nature* **352**, 530 (1991); F. Lozano, C. Rada, J. Jarvis, C. Milstein, *Ibid.* **363**, 271 (1993).
27. M. Pearse *et al.*, *Proc. Natl. Acad. Sci. U.S.A.* **85**, 6082 (1988).
28. M. Schlissel and D. Baltimore, *Cell* **58**, 1001 (1989).
29. Primer sequences, PCR conditions, and probes were as follows: V_κ degenerate, as in (*28*); $J_\kappa 4$: 5′-GGATCTTCTATTGATGCACAGGTTGCCAGG-3′; $J_\kappa 4$ probe: 5′-GGCTCGGGGACAAAGTTGGAA-ATAAAACGTAAG-3′; 24 cycles of 30 min at 94°C, 30 min at 60°C, and 30 min at 72°C.
30. We thank M. Schlissel for help with the LM-PCR protocol and the Nussenzweig laboratory for critically reviewing the manuscript. Supported by NIH grant AI33890 (M.C.N.) and a Deutche Forschungsgemeinschaft grant (K.R.). M.C.N. is an associate investigator in the Howard Hughes Medical Institute.

30 June 1997; accepted 12 August 1997

V(D)J Recombinase Activity in a Subset of Germinal Center B Lymphocytes

Shuhua Han,* Stacey R. Dillon,* Biao Zheng, Michiko Shimoda, Mark S. Schlissel, Garnett Kelsoe†

Reexpression of the V(D)J recombinase-activating genes *RAG1* and *RAG2* in germinal center B cells creates the potential for immunoglobulin gene rearrangement and the generation of new antigen receptor specificities. Intermediate products of V(D)J recombination are abundant in a subset of germinal center B cells, demonstrating that the κ immunoglobulin light-chain locus becomes a substrate for renewed V(D)J recombinase activity. This recombinationally active cell compartment contains many heavy-chain VDJ rearrangements that encode low-affinity or nonfunctional antibody. In germinal centers, secondary V(D)J recombination may be induced by diminished binding to antigen ligands, thereby limiting abrupt changes in receptor specificity to B cells that are usually eliminated from the germinal center reaction. This restriction preserves efficient antigen-driven selection in germinal centers while allowing for saltations in the somatic evolution of B cells.

The primary antibody repertoire is created during the pre-B and immature stages of B lymphogenesis by V-to-J recombination in the κ and λ light-chain (L-chain) loci (*1*) and by tolerance mechanisms that either purge newly generated, autoreactive B cells by apoptosis (*2*) or render them harmless by a process of secondary V(D)J rearrangements known as receptor editing (*3*). Remarkably, during the immune response known as the germinal center (GC) reaction, some B cells begin to transcribe λ5, a component of the pre-B cell receptor complex (*4, 5*), express the RAG1 and RAG2 V(D)J recombinase proteins (*5*), and become highly sensitive to receptor-induced apoptosis (*6*). This broad recapitulation of lymphocyte development and the availability of V(D)J recombinase suggests that at least some GC B cells might also undergo secondary immunoglobulin (Ig) gene rearrangements.

GCs are established by the focal proliferation of mature, antigen-reactive lymphocytes in the B cell zones of secondary lymphoid tissues (*7*). They are crucial for immunological memory in the B cell compartment and are primary sites for the V(D)J hypermutation and cellular selection necessary for affinity maturation of antibody responses (*8*). B cells that enter nascent GCs bear IgM and IgD on their surface and express the low-affinity IgE Fc receptor, CD23 ($CD23^+$). With time, GC B cells cease to express membrane IgD and CD23 and acquire a characteristic phenotype that includes avid binding of peanut agglutinin and the GL-7 antibody (PNA^{hi}, $GL\text{-}7^+$), upregulation of the Fas death trigger ($CD95^+$), and increased expression of CD24 ($CD24^{hi}$) (*7, 9*). This core phenotype remains stable during the primary GC reaction.

Although the majority of splenic GC B cells ($GL\text{-}7^+$, $CD95^+$, $CD24^{hi}$) express amounts of B220 (CD45R) typical of mature B lymphocytes ($B220^{hi}$), a population of GC B lymphocytes that expresses B220 in amounts similar to pre-B cells ($B220^{lo}$) appears by day 10 to 12 after immunization (*10*) and expands, eventually constituting as much as half (25 to 53%) of all $GL\text{-}7^+$ B lymphocytes (Fig. 1). Proliferation, as measured by incorporation of the nucleotide analog, 5-bromo-2′-deoxyuridine (BrdU), is equivalent in $B220^{lo}$ and $B220^{hi}$ GC cells and consistent with the rapid proliferation of GC B lymphocytes (*7, 11*).

The delayed appearance of the $B220^{lo}$ population of GC B cells is similar to the kinetics of local RAG expression (*5*). To compare the distribution of recombinase and λ5 expression in $B220^{lo}$ and $B220^{hi}$ GC cell populations, we purified 1×10^4 follicular ($GL\text{-}7^-$, $B220^+$), GC ($GL\text{-}7^+$, $B220^+$), and $B220^{lo}$ and $B220^{hi}$ GC ($GL\text{-}7^+$) cells from the splenocytes of immunized C57BL/6 mice by fluorescence-activated cell sorting (FACS) (*12*). A reverse transcriptase–dependent polymerase chain reaction (RT-PCR) was then used to determine the presence of RAG1, RAG2, λ5, and hypoxanthine-guanine phosphoribosyl transferase (HPRT) mRNA in aliquots of each sorted population (*13*). Whereas equivalent amounts of HPRT mRNA were present in all cell samples (Fig. 2D), recombinase and λ5 message (Fig. 2, A to C) were present in $B220^+$ GC cells but could not be detected in follicular B lymphocytes. Among GC cells, RAG and λ5 transcripts were largely confined to the $B220^{lo}$ compartment. Transcription of the *RAG* and λ5 genes is correlated with the $B220^{lo}$ GC cell phenotype.

To determine if V(D)J recombination was active in GC B cells, we designed a locus-specific, ligation-mediated PCR (LM-PCR) assay to detect double-stranded (ds) recombination signal sequence (RSS) breaks in the Ig κ locus (Fig. 3A). These blunt, 5′-phosphorylated, ds breaks at RSSs are intermediates of V(D)J recombination and depend on the unique enzymatic activity of RAG1 and RAG2 (*14*). Purified DNA samples were ligated to an unphosphorylated linker oligonucleotide (BW) containing one blunt and one overhanging end. RSS breaks 3′ to a prior V-to-J_κ rearrangement were then amplified by PCR, using a linker-specific primer (BW-H) and a primer, $V_\kappa B$ or $V_\kappa S$, that hybridizes to most V_κ gene segments (*15, 16*). A fraction of this initial PCR product was then amplified in a second round of PCR using BW-H

S. Han, B. Zheng, M. Shimoda, G. Kelsoe, Department of Microbiology and Immunology and Program in Molecular and Cell Biology, University of Maryland School of Medicine, 655 West Baltimore Street, Baltimore, MD 21201, USA.
S. R. Dillon and M. S. Schlissel, Departments of Medicine, Molecular Biology and Genetics, and Oncology, The Johns Hopkins University School of Medicine, Baltimore, MD 21205, USA.

*These authors contributed equally to this work.
†To whom correspondence should be addressed. E-mail: gkelsoe@umabnet.ab.umd.edu

and primers annealing 5′ of $J_\kappa 2$, $J_\kappa 4$, or $J_\kappa 5$. Because the distance from unrearranged Vκ gene segments to the Jκ cluster is too great for amplification, this assay preferentially detects RSS breaks associated with replacement rearrangements.

To search for active, secondary Ig κ rearrangement in GC B cells, we immunized mice with chicken γ-globulin (CGG) (*10*). At 8 and 16 days after immunization, specific B cell populations were purified by cell sorting (*12*), and DNA from sorted lymphocytes and control cells was subjected to the LM-PCR assay (*17*). Although amplification of a nonrearranging control gene, CD14, was comparable in all samples (Fig. 3B, upper panel) and dsDNA breaks at J_κ RSSs were absent in 3T3 fibroblasts and thymocytes, distinctive patterns of RSS breaks appeared in the sorted cell populations (Fig. 3B, lower panel). Breaks were abundant in the splenocytes of 3-day-old mice because of the high frequency of immature B cells present in the neonatal spleen (*16*), but were undetectable in spleens from unimmunized aged mice. In immunized, young adult mice, we found $J_\kappa 2$ RSS breaks in both resting and antigen-activated cell populations, but $J_\kappa 4$ and $J_\kappa 5$ RSS breaks were present only in cell samples containing activated lymphocytes. $J_\kappa 2$ RSS breaks in resting cells probably derive from maturing B cells (IgD^{lo}, $CD23^-$, $CD24^{hi}$) present in splenic T cell areas (*18*). In contrast, $J_\kappa 4$ or $J_\kappa 5$ RSS breaks were present in a single sample of GC ($CD43^-$ $GL\text{-}7^+$) B cells recovered 8 days after immunization and in all $GL\text{-}7^+$ GC cells taken 16 days after immunization. These $J_\kappa 4$ and $J_\kappa 5$ RSS breaks were present largely, if not exclusively, within $B220^{lo}$ GC B cells. Hence, the GC B cells that contain abundant amounts of RAG1 and RAG2 mRNA (Fig. 2) also contain the intermediate DNA products of V(D)J recombination. Few or no RSS breaks were detected in $B220^{hi}$ GC cells or $CD43^{hi}$ plasmacytes, even though $J_\kappa 2$ RSS breaks were present in unactivated, follicular B cells ($B220^+$, $GL7^-$). The dearth of RSS breaks in $B220^{hi}$ GC cells and plasmacytes is most likely the result of antigen-driven cellular proliferation, because RSS breaks are repaired upon reentry into the cell cycle (*19*). Thus, RSS breaks in the rapidly proliferating $B220^{lo}$ GC population indicates ongoing V(D)J recombination. Amplification of RSS breaks (*17*) in decreasing amounts of DNA from B-lineage ($CD19^+$) bone marrow cells, $B220^{lo}$ and $B220^{hi}$ GC cells, and the temperature-sensitive pre-B cell line 103-bcl2 (*20*) indicated that replacement rearrangements are abundant in the $B220^{lo}$ GC compartment. Secondary V_κ-to-$J_\kappa 2$ rearrangements could be detected in as little as 0.8 ng of DNA from bone marrow and $B220^{lo}$ GC cells, whereas 5- to 25-fold more template was required to detect RSS breaks in induced 103-bcl2 cells and $B220^{hi}$ GC cells, respectively.

To determine if $B220^{lo}$ and $B220^{hi}$ GC cells express comparable antigen receptors, mice were immunized with CGG substituted with the (4-hydroxy-3-nitrophenyl)acetyl (NP) hapten (*10*). Initially, NP activates B cells bearing the λ1 L-chain and heavy-chains (H-chains) encoded by the V23, CH10, C1H4, or V186.2 V_H gene segments (*21*, *22*); later, the response becomes dominated by cells that express the higher affinity V186.2 rearrangement (*22*). NP-reactive B cells that contain V_H V186.2

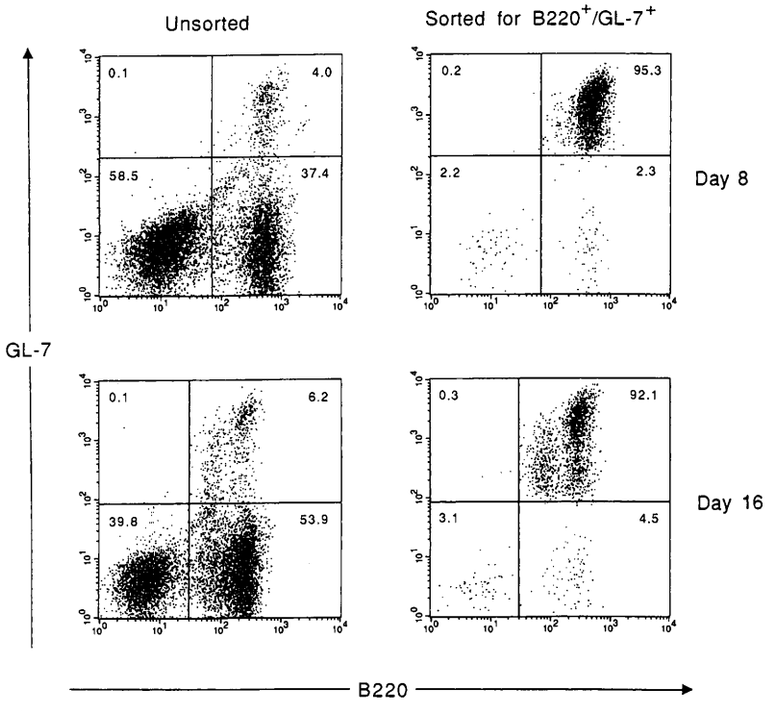

Fig. 1. Flow cytometric analysis of splenic germinal center (GC) B cells from C57BL/6 mice at 8 and 16 days after immunization with CGG. Dissociated splenocytes were stained with anti-B220–FITC and GL-7–biotin followed by streptavidin-PE, as described (*5*). Two subpopulations, $B220^{lo}$ and $B220^{hi}$, of GC cells are present in late phase (day 16) GCs but not at early time points (day 8) after immunization.

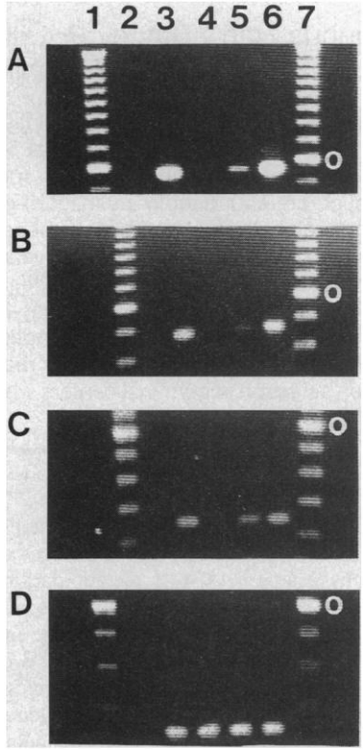

Fig. 2. RT-PCR assays to detect the expression of *RAG1*, *RAG2*, and λ*5* in GC B cell populations. Splenic cells recovered from immunized C57BL/6 mice at day 16 were stained with anti-B220–FITC and GL-7–biotin (*11*). $B220^{lo}/GL\text{-}7^+$, $B220^{hi}/GL\text{-}7^+$, and $B220^+/GL\text{-}7^-$ B cells were sorted into TRIzol, and RT-PCR was performed as described (*12*) to determine the presence of mRNA for RAG1 (**A**), RAG2 (**B**), and λ5 (**C**) in different cell populations. HPRT (**D**) was used as a control to ensure the amounts of mRNA recovered in each sample were equivalent. In addition, RNA was purified from bone marrow (BM) of young adult C57BL/6 mice and used as a control. After 35 amplification cycles, PCR products were electrophoresed on agarose gels and detected by staining with ethidium bromide. Lane 1, molecular size markers; lane 2, control (no reverse transcriptase, 1×10^4 BM cells); lane 3, 1×10^4 BM cells; lane 4, 1×10^4 $GL\text{-}7^-B220^+$ B cells; lane 5, 1×10^4 $B220^{hi}$ $GL\text{-}7^+$ GC cells; lane 6, 1×10^4 $B220^{lo}$ $GL\text{-}7^+$ GC cells; lane 7, molecular size markers. The open circle (O) indicates a molecular size of 600 bp.

rearrangements with a tyrosine-rich motif (YYYGS) (*23*) in the third complementarity-determining region (CDR3), and mutations that yield tryptophan → leucine (W→L) replacements at position 33 strongly bind the NP hapten and are considered highly selected (*24*).

Sequence analysis of randomly chosen VDJ fragments amplified (*25*) from B220^{lo} (n = 20) and B220^{hi} (n = 20) GC cells showed that these cell populations express very different collections of antigen receptors (Table 1). The B220^{hi} population is enriched for V_H gene rearrangements and mutations consistent with avid NP-binding (*26*). In contrast, VDJ fragments amplified from the B220^{lo} population of GC cells exhibited few characteristics of high-affinity, NP-specific antibodies. Nearly one-third (30%) of VDJ rearrangements from B220^{lo} GC cells contained V_H gene segments (V23, C1H4, CH10, 24.8, and 593.3) that are common in early, NP-reactive GCs but encode antibodies with low affinities for this hapten (*22*, *26*). These data suggest that although B220^{hi} GC cells strongly bind antigen, the B220^{lo} population consists of lower affinity B lymphocytes that no longer compete effectively for antigen (*7*). This conclusion was tested by transfecting 14 productive and representative VDJ rearrangements from B220^{hi} (n = 8) and B220^{lo} (n = 6) GC cells into the J558L cell line (*27*). The association constant (K_a) of each transfectoma antibody for the NP hapten was then measured by fluorescence quenching (*26*). As expected, the average K_a (2.4×10^6 M^{-1}) for the B220^{hi} group was significantly greater than that of B220^{lo} cells (8.0×10^4 M^{-1}).

Germinal centers support a stage in B cell development where renewed V(D)J recombinase expression in B220^{lo} cells (Fig. 1) drives replacement rearrangements in the Ig L-chain loci (Fig. 3). Secondary V(D)J rearrangement and revision of receptor specificity also occurs in some autoreactive, immature B cells in the bone marrow (*3*). Although GC B cells express many properties of pre-B and immature B cells, the V_κ-to-J_κ recombination we observed is not ectopic lymphogenesis. GCs were founded by antigen-reactive B cells bearing high amounts of IgD and CD23 on their surface (*9*), and mutated H-chain (Table 1) and λ1 L-chain gene rearrangements were present in both B220^{hi} and B220^{lo} GC cells. In addition, the signals that drive secondary Ig gene rearrangements in bone marrow and GC B cells appear to differ. Receptor editing in immature B cells is believed to be in response to self-reactivity (*3*). In GCs, experimental models of autoreactivity induce rapid apoptosis (*6*) without superinduction of RAG1 protein (*28*). Instead, patterns of V_H gene segment usage, the dearth of affinity-enhancing mutations in B220^{lo} GC cells (Table 1), and affinity measurements of transfectant antibodies imply that receptor

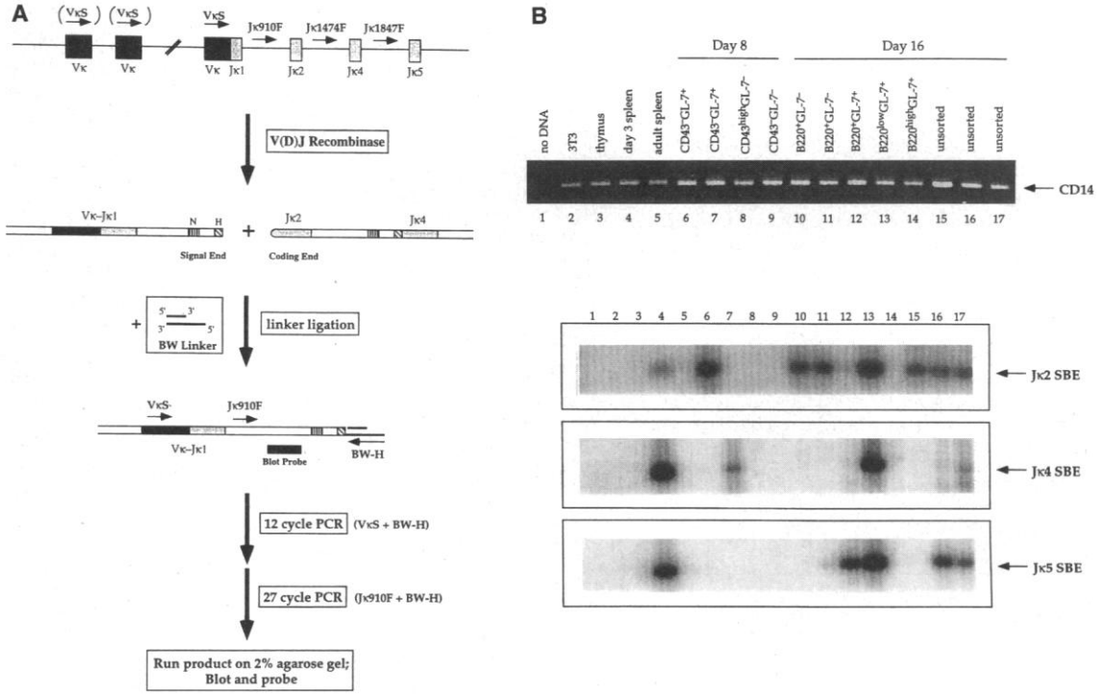

Fig. 3. LM-PCR assay to detect secondary V(D)J recombination in GC B cells. (**A**) Diagram of the LM-PCR assay designed to detect DNA breaks associated with replacement rearrangements at the Ig κ locus. The κ locus is shown with a primary V_κ-J_κ1 rearrangement and, as an example, an attempted secondary rearrangement to J_κ2. The PCR primers used to detect RSS breaks at J_κ2, J_κ4, and J_κ5 (J_κ3 is a nonfunctional pseudogene) are also depicted (J_κ910F, J_κ1474F, J_κ1847F, respectively). Hypothetical broken DNA molecules corresponding to signal ends—with the nonamers (N) and heptamers (H) depicted as hatched boxes—are shown alongside the BW linker, an unphosphorylated blunt-ended 25-mer with a 14-nucleotide 5′ overhang. The BW linker ligates to RAG-dependent, double-stranded signal sequence breaks, which are blunt and 5′-phosphorylated (*15*). BW linker-ligated DNA is subjected to two rounds of PCR amplification, as described (*18*). PCR products were electrophoresed on 2% agarose gels, blot-transferred to nylon membranes, probed with a radiolabeled oligonucleotide (J_κ1-2, J_κ1568F, or J_κ2000F for breaks at J_κ2, J_κ4, or J_κ5, respectively) internal to the PCR primers as shown, and analyzed on a phosphorimager. (**B**) RSS breaks in the Ig κ locus are present in DNA from sorted GC B cells. Seven-month-old C57BL/6 mice were immunized with CGG in alum. At day 16, splenocytes isolated from these mice were sorted to collect GL-7$^+$ GC B cells, GL-7$^-$ follicular B cells, and B220^{lo} and B220^{hi} GC populations. Two-month-old C57BL/6 mice were also used to obtain CD43$^+$/GL-7$^-$ plasmacytes or CD43$^-$/GL-7$^+$ GC cells at day 8 after immunization. Analyses after sorting revealed that the purity of the GC cells was >90%, whereas the follicular cells were >95% pure. DNA from sorted populations was purified, dissolved in a small volume of H_2O, then ligated overnight to the BW linker (*18*). An aliquot of each sample (~20 ng) was tested in a control PCR (*18*) using primers for the nonrearranging CD14 locus, to ensure that a similar amount of DNA was present in each sample (upper panel). LM-PCR using primers designed to detect RSS breaks upstream of J_κ2, J_κ4, and J_κ5 was performed in the absence of DNA template (lane 1), or with ~20 ng of DNA isolated from the following cells: NIH 3T3 fibroblasts (lane 2); thymocytes (lane 3); day-3 newborn spleen (lane 4); unimmunized adult spleen (lane 5); day-8 sorted CD43$^-$GL-7$^+$ GC B cells (lanes 6 and 7), CD43^{hi}GL-7$^-$ plasma cells (lane 8), and CD43^{lo}GL-7$^-$ B cells (lane 9); and day-16 sorted B220$^+$GL-7$^-$ follicular B cells (lanes 10 and 11), B220$^+$GL-7$^+$ GC B cells (B220^{lo} and B220^{hi}, lane 12), B220^{lo}GL-7$^+$ (lane 13), B220^{hi}GL-7$^+$ (lane 14), and stained but unsorted splenocytes (lanes 15 to 17).

revision in GCs is induced by diminished or lost antigen-binding. V(D)J recombination in the B220^{lo} subset of GC B cells limits L-chain replacement and the consequent saltations in receptor specificity to a cell compartment that is normally eliminated from GCs (*7*). The improbable genetic experiment of receptor revision is confined to B cells that are destined for programmed cell death.

However improbable, we believe that replacement rearrangements in GC B cells must confer significant benefit to immune function, because recombinase activity carries appreciable risks, including malignant transformation by illegitimate recombination (*29*). Replacement rearrangements may rescue failing GC B cells by revising low-affinity receptors or those debilitated by mutation. Indeed, pairings of H- and L-chains consistent with receptor revision in GCs have been observed in the response of BALB/c mice to the 2-phenyl oxazolone hapten (*30*). More speculatively, saltations in receptor specificity may provide new avenues for clonal evolution, leading to affinities that could not be achieved by mutation alone.

In response to exogenous antigen, the GC microenvironment allows B cells to reactivate the fundamental event of lymphocyte development, V(D)J recombination. Immunoglobulin gene rearrangements in GC B cells that restore or enhance antigen-binding would be analogous to those in immature B lymphocytes that abolish autoreactivity (*3*): in each case, the recombinase machinery is reactivated to preserve cells that would otherwise be lost to the immune response.

Table 1. Comparison of VDJ rearrangements from B220^{hi} and B220^{lo} GC (GL-7$^+$) cells. B220^{hi} and B220^{lo} GL-7$^+$ cells were isolated by FACS as described (*11*).

	GC (GL-7$^+$) cells	
	B220^{hi}	B220^{lo}
V_H Usage (%)*		
V186.2	100	70
Related	0	30
P:nP†	20:0	17:3
YYYGS CDR3 (%)	25	5
Position 33 W → L (%)	47	0
Avg. freq. mutation (%)‡	2.0	0.6

*VDJ rearrangements were amplified from the genomic DNA of sorted cell populations as described (*26*). Related V_H gene segments included: V23, C1H4, CH10, 24.8 and 593 (*22*). †Productive (P) VDJ rearrangements were defined by in-frame V-to-D-to-J junctions. Nonproductive (nP) joins were not in-frame. One nP VDJ sequence resulted from a 215-bp insertion into a VDJ rearrangement of the V186.2 gene. ‡Mutations were present (range = 3 to 11; average = 5.8 ± 2.4) in all VDJ rearrangements amplified from sorted B220^{hi} GC cells; no mutation introduced a termination codon. Fourteen (70%) VDJ rearrangements from B220^{lo} GCs contained point mutations (range = 0 to 4; average = 1.7 ± 1.6); two rearrangements contained point mutations that produced termination signals.

REFERENCES AND NOTES

1. H. Karasuyama, A. Rolink, F. Melchers, *Adv. Immunol.* **63**, 1 (1996); K. Rajewsky. *Nature* **381**, 751 (1996).
2. C. Goodnow, *Annu. Rev. Immunol.* **10**, 489 (1992).
3. M. Z. Radic and M. Zouali, *Immunity* **5**, 505 (1996).
4. U. Grawunder *et al.*, *ibid.* **3**, 601 (1995); N. Sakaguchi and F. Melchers, *Nature* **324**, 579 (1986).
5. S. Han, B. Zheng, D. G. Schatz, E. Spanopoulou, G. Kelsoe, *Science* **274**, 2094 (1996); M. Hikida *et al.*, *ibid.*, p. 2092.
6. S. Han, B. Zheng, J. Dal Porto, G. Kelsoe, *J. Exp. Med.* **182**, 1635 (1995); B. Pulendran *et al.*, *Nature* **375**, 331 (1995); K. M. Shokat and C. C. Goodnow, *ibid.*, p. 334.
7. I. C. M. MacLennan, *Annu. Rev. Immunol.* **12**, 117 (1994); G. Kelsoe, *Adv. Immunol.* **60**, 267 (1995).
8. R. F. Coico, S. Boghal, G. J. Thorbecke, *J. Immunol.* **131**, 2254 (1983); C. Berek, A. Berger, M. Apel, *Cell* **67**, 1121 (1991); J. Jacob, G. Kelsoe, K. Rajewsky, U. Weiss, *Nature* **354**, 389 (1991); S. Han *et al.*, *J. Immunol.* **155**, 556 (1995).
9. C. Miller, G. Kelsoe, S. Han, *Aging Immunol. Infect. Dis.* **5**, 249 (1994); H. Kimoto *et al.*, *Eur. J. Immunol.* **27**, 268 (1997); D. Cerasoli and G. Kelsoe, unpublished observations.
10. C57BL/6 female mice (Jackson ImmunoResearch Labs) were kept in sterile microisolators. All the mice, except for those used for DNA break assays (Fig. 3), were young adults (8 to 10 weeks old). Mice were immunized intraperitoneally with 100 μg of (4-hydroxy-3-nitrophenyl)acetyl–chicken γ-globulin (NP-CGG) or CGG precipitated in alum (*6*). Spleens of immunized mice were taken at times indicated after immunization and dissociated into single-cell suspensions.
11. Cellular proliferation was determined at 16 days after immunization with CGG (*10*). Mice were injected intraperitoneally with 2 mg of BrdU 3 hours before being killed. Splenic B cell populations were then isolated by FACS; purified (>95%) populations of follicular (B220$^+$, GL-7$^-$) and B220^{hi} and B220^{lo} GC (GL-7$^+$) B cells were centrifuged onto glass slides for immunohistological enumeration of BrdU$^+$ cells. Frequencies of cells exhibiting nuclear incorporation of BrdU: follicular B cells <2%; B220^{hi} GC cells = 26.4 ± 7.6%; B220^{lo} GC cells = 29.3 ± 4.0%.
12. Single-cell suspensions were prepared from spleens of naïve and immune mice and were incubated with purified anti-mouse CD32/CD16 (PharMingen, San Diego, CA) to block antibody binding to Fc receptors. The spleen cells were then stained with anti-B220–fluorescein isothiocyanate (FITC) and GL-7–biotin followed by streptavidin-phycoerythrin (PE). Stained cells were processed by a dual-laser flow cytometer (Becton Dickinson) and sorted either into TRIzol (Gibco, Life Technologies) for RT-PCR analysis and genomic DNA purification, or into cold medium for LM-PCR assays and BrdU detection. Reanalysis of sorted fractions showed purities of 90 to 99%. CD43$^+$/GL-7$^-$ B cells were prepared by magnetic cell sorting before FACS. T cells, granulocytes, macrophages, and IgD$^+$ B cells were depleted with biotinylated antibodies (PharMingen) to Thy-1.2, Gr-1, Mac-1, and IgD followed by incubation with streptavidin beads (Miltenyi Biotec, Auburn, CA). Depleted cell populations were then stained with anti-CD43-PE (PharMingen) and GL-7-FITC (PharMingen) and purified by cell sorting, as above, to obtain CD43$^+$/GL-7$^-$ plasmacytes or CD43$^-$/GL-7$^+$ GC B cells.
13. Total RNA was recovered from limited numbers of sorted cells using TRIzol reagent (Gibco). After ethanol precipitation, all RNA of each sample was used for first-strand cDNA synthesis in a total volume of 20 μl, using a SuperScript kit (Gibco). We used 2 μl of the cDNA solution for PCR amplification in 50 μl volume reaction with Taq polymerase (Gibco). The primers used for *RAG1*, *RAG2*, and Hprt have been described previously (*5*). The primers for λ5 were 5′-ACTGGTCAGATATCAGTGTC-3′ for reverse transcription; 5′-TTGGGTCTAGTGGATGGTGTCC-3′ and 5′ CTGACCTAGGATTGTGAGCTGGGT-3′ for PCR amplification.
14. M. Schlissel, A. Constantinescu, T. Morrow, M. Baxter, A. Peng, *Genes Dev* **7**, 2520 (1993); J. F. McBlane *et al.*, *Cell* **83**, 387 (1995).
15. M. Schlissel and D. Baltimore, *Cell* **58**, 1001 (1989).
16. A. Constantinescu and M. Schlissel, *J. Exp. Med.* **185**, 609 (1997).
17. DNA was purified and dissolved in H_2O at an approximate concentration of 5 ng/μl, as estimated from the number of cells recovered. The BW linker was prepared as previously described (*15*). DNA was subjected to linker ligation in a 40-μl ligation mixture containing ligation buffer (Boehringer Mannheim), 40 pmol of BW linker, and 2 U of T4 DNA ligase and was incubated overnight at 16°C. The reaction was then mixed with 100 of μl of PCR-L buffer [10 mM tris (pH 8.8), 50 mM KCL, 0.25% Tween-20, and 0.25% Nonidet P-40] and heated to 95°C for 15 min before PCR. The primary amplification consisted of 12 cycles each of 94°C for 1 min and 66°C for 2.5 min, using the linker-specific primer BW-H and the $V_κ$-specific primers $V_κ$B or $V_κ$S. We used 1 μl of the primary reaction for a second amplification with BW-H and a nested, locus-specific primer ($J_κ$910F for $J_κ$2, $J_κ$1474F for $J_κ$4, or $J_κ$1847F for $J_κ$5) consisting of 27 PCR cycles under the same conditions. A 27-cycle control reaction (identical conditions) was also run, using the CD14-L and CD14-R primers and ~20 ng of linker-ligated template DNA. One-half of the final PCR product was analyzed by electrophoresis on a 2% agarose gel, then blotted as described (*15*). Blots were hybridized to ^{32}P end-labeled, locus-specific internal oligonucleotides ($J_κ$1-2 for $J_κ$2, $J_κ$1568F for $J_κ$4, or $J_κ$2000F for $J_κ$5) and analyzed with a phosphorimager using ImageQuant software (Molecular Dynamics). Oligonucleotide sequences: $J_κ$910F, 5′-GGGAATAGGCTAGACATGTTCTC-3′; $J_κ$1474F, 5′-GGTCCCATTGTGTCCTTTGTATGAGTTTGTGG-3′; $J_κ$1847F, 5′-GCCATTCCTGGCAACCTGTGCATCA-3′; $J_κ$1-2, 5′-GTGTCCCTTCACTCAACCCCCATAC-3′; $J_κ$1568F, 5′-TCTAGCTACTGTACAAGCTGAGCAAACAGAC-3′; and $J_κ$2000F, 5′-TAGTTGGACTGGCTTCACAGGCA-3′. The sequences of BW-1, BW-2, BW-H, CD14-L, CD14-R, $V_κ$B, and $V_κ$S have been published (*14–16*).
18. D. M. Allman, S. E. Ferguson, V. M. Lentz, M. P. Cancro, *J. Immunol.* **151**, 4431 (1993); R. J. Cornall, C. C. Goodnow, J. G. Cyster, *Curr. Opin. Immunol.* **7**, 804 (1995); J. G. Cyster *et al.*, *Nature* **381**, 325 (1996).
19. D. A. Ramsden and M. Gellert, *Genes Dev.* **9**, 2409 (1995).
20. Y.-Y. Chen, L. C. Wang, M. S. Huang, N. Rosenberg, *ibid.* **8**, 688 (1994).
21. H. Gu, D. Tarlinton, W. Muller, K. Rajewsky, I. Foster, *J. Exp. Med.* **173**, 1357 (1991).
22. J. Jacob, J. Przylepa, C. Miller, G. Kelsoe, *ibid.* **178**, 1293 (1993).
23. Single-letter abbreviations for the amino acid residues are as follows: G, Gly; L, Leu; S, Ser; W, Trp; and Y, Tyr.
24. C. Kocks and K. Rajewsky, *Annu. Rev. Immunol.* **7**, 537 (1989).
25. Genomic DNA was isolated from different cell populations sorted into TRIzol reagent (Gibco) after chloroform extraction. After ethanol precipitation, the DNA was solubilized in 8 mM NaOH and then adjusted with Hepes buffer to a pH of 7.2 to 7.4. PCR reactions were performed as described (*22*) using *Pfu* polymerase. Briefly, the initial round of 40 amplification cycles used primers complementary to genomic DNA 5′ of the transcriptional start site of the V186.2 V_H gene segment and to a region in the J_H2-J_H3 intron. We reamplified 2-μl aliquots of this reaction mixture for an additional 40 cycles using a second set of nested primers complementary to the first 20 nucleotides of the V186.2 exon and to the terminal portion of the J_H2 element. Amplified products were ligated into the plasmid, pBSK, and then electroporated into competent DH5α bacteria. Recombinant colonies were screened with a ^{32}P-labeled oligonucleotide corresponding to amino acid positions 70 through 74 of the V186.2 gene segment. DNA from positive clones was subjected to sequencing on an Applied Biosystems 373A automated DNA sequencer.
26. J. Dal Porto, A. Haberman, M. Shlomchik, G. Kelsoe, in preparation. In this sample VDJ fragments from B220^{hi} GC cells, three hybrid gene sequences (*22*) were iden-

tified; each consisted of an in-frame exchange of 9 to 48 base pairs (bp) from the C1H4 gene segment into unrelated rearrangements of V186.2. In the sample from B220^{lo} GC cells, only a single V_H V23 rearrangement encoded the YYYGS motif in CDR3, and three rearrangements, all V186.2, were not in-frame. Two of these nonproductive (nP) rearrangements resulted from incomplete codons at the V-D-J junction, whereas the third contained a complex 215-bp insertion of DNA from the V186.2 and V_H 165.1 gene segments. Two hybrid sequences were present: the 215-bp insert described earlier and an in-frame exchange of 30 bp from the C1H4 exon into a productive V186.2 rearrangement.

27. C. Miller and G. Kelsoe, *J. Immunol.* **155**, 3377 (1995).
28. S. Han and G. Kelsoe, unpublished data.
29. A. Bakhshi *et al.*, *Proc. Natl. Acad. Sci. U.S.A.* **84**, 2396 (1987); Y. Tsujimoto, E. Louie, M. M. Bashir, C. M. Croce, *Oncogene* **2**, 347 (1988); F. Cotter, C. Price, E. Zucca, B. D. Young, *Blood* **76**, 131 (1990).
30. G. M. Griffiths, C. Berek, M. Kaartinen, C. Milstein, *Nature* **312**, 271 (1984).

31. We thank J. Cerny and A. Perelson for their review of this manuscript. Supported in part by USPHS grants HL48722 and AI40227 (M.S.S.) and AI24335, AG10207, and AG13789 (G. K). S.R.D. is a recipient of an Arthritis Foundation Postdoctoral Fellowship, M.S.S. acknowledges the support of a Leukemia Society Scholarship and G.K. received funding from the Jeanne M. and Joseph P. Sullivan Foundation and the Santa Fe Institute.

9 July 1997; accepted 19 August 1997

TECHNICAL COMMENT

BMP Expression in Duck Interdigital Webbing: A Reanalysis

Ed Laufer
Department of Genetics, Harvard Medical School, Boston, MA 02115, USA
Sandrine Pizette
Hongyan Zou
Program in Molecular Biology, Memorial Sloan-Kettering Cancer Center, New York, NY 10021, USA
Olivia E. Orozco
Department of Genetics, Harvard Medical School
Lee Niswander
Program in Molecular Biology, Memorial Sloan Kettering Cancer Center

In 1996, two of us (H.Z. and L.N.) reported that expression of a dominant-negative form of BMP receptor (*dnBMPR-IB*) in the embryonic chick hindlimb inhibited interdigital apoptosis and led to webbing of the digits (*1*) (BMPs are signaling molecules of the transforming growth factor–β superfamily). The importance of BMP signaling in regulating interdigital cell death has recently been confirmed by the use of an activated *BMPR-IB* retrovirus (*2*) and by application of BMP protein (*3*, *4*).

It was also stated in this report (*1*) that *BMP2*, *4*, and *7* RNA expression was not detected in the duck interdigit. This result implied that the webbing in the hindlimb of ducks is a consequence of the absence of BMP expression in the duck embryo. After publication of the report (*1*), to explore this issue further, subsequent in situ hybridizations were carried out with the use of a modification (*5*) of an existing whole mount, in situ protocol. Results from our two different laboratories now indicate that *BMP2*, *4*, and *7* are in fact expressed in the duck interdigit in a pattern similar to that of the chick interdigit (Fig. 1). The in situ protocol we used, in contrast with the protocol followed in the original study (*1*), included use of (i) a higher proteinase K concentration (30 to 70 μg/ml rather than 5 μg/ml), (ii) BCIP/NBT (*6*) as a color detection substrate rather than Boehringer-Mannheim purple AP substrate, and (iii) a TWEEN-20 concentration of 1% rather than 0.1% during the color substrate reaction. In combination, these modifications resulted in a greater sensitivity in detecting interdigital expression of *BMP2*, *4*, and *7* in late-stage embryonic limbs. This result has been confirmed for *BMP7* by nonradioactive in situ hybridization to frozen tissue sections (*7*). Therefore, we (H.Z. and L.N.) must withdraw the earlier finding that the duck interdigit lacks BMP expression and regret any inconvenience the earlier conclusions may have caused.

REFERENCES AND NOTES

1. H. Zou and L. Niswander, *Science* **272**, 738 (1996).
2. H. Zou, R. Wieser, J. Massagué, L. Niswander, *Genes Devel.* **11**, 2191 (1997).
3. Y. Yokouchi *et al.*, *Development* **122**, 3725 (1996).
4. D. Macias *et al.*, *ibid.* **124**, 1109 (1997).
5. Whole mount in situ hybridizations were performed as described by R. D. Riddle *et al.* [*Cell* **75**, 1401 (1993)], except that the temperature of all hybridizations and post-hybridization washes was 60°C and the proteinase K (PK) conditions were varied. Standard 1× PK is nominally 10μg/ml for 15 min at room temperature. However, we have noted batch variation in the specific activity of PK, and the conditions must therefore be titrated for each batch. Typically, 1× PK treatment results in the removal of most or all of the signal from s22 limb bud AERs, and strong mesenchymal signal for genes such as *BMP2* or *Sonic hedgehog*. Maximal AER staining is usually seen around 1/4× PK. Older embryos often require substantially more PK treatment to reveal strong mesenchymal signals (up to 10× for 9-day-old embryonic limbs). In the experiments described here, PK conditions were independently optimized for visualization of interdigital BMP expression in both chick and duck limb buds. Following PK digestion, stage-matched chick and duck embryos were combined into a single vial and treated together for the remainder of the protocol. NBT/BCIP reactions were performed at room temperature for varying amounts of time (typically 1.5 to 3 hours), until a strong interdigital signal was observed. All of the probes were derived from the chick BMP genes, as described in Zou and Niswander (*1*).
6. BCIP, 5-bromo-4-chloro-3-indolyl phosphate; NBT, nitro blue tetrazolium; both available from Sigma.
7. E. Laufer *et al.*, unpublished data.
8. V. Hamburger and H. L. Hamilton, *J. Exp. Morphol.* **88**, 49 (1951).

20 August 1997; accepted 9 September 1997

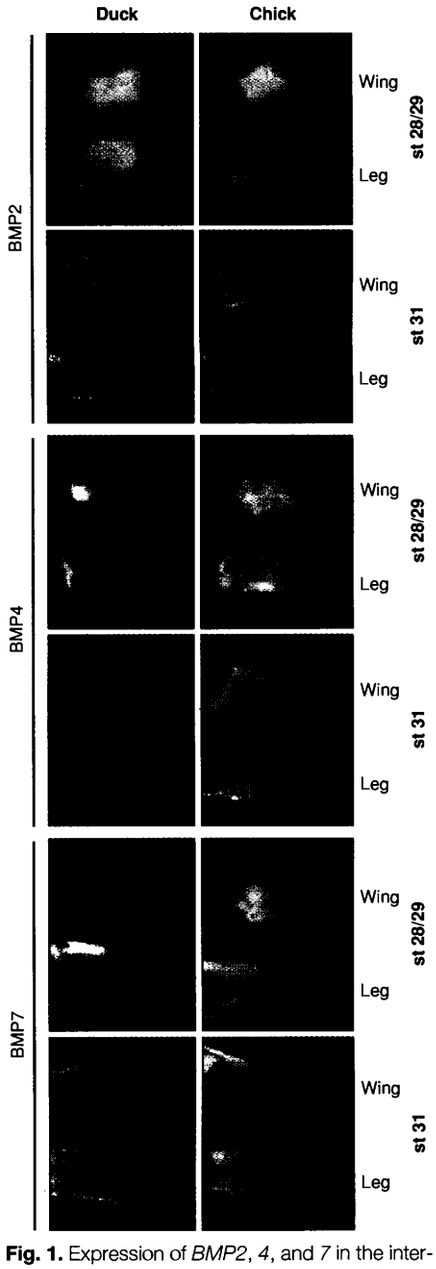

Fig. 1. Expression of *BMP2*, *4*, and *7* in the interdigital regions of chick and duck limbs. Expression of each gene was detected by whole mount in situ hybridization to stage 28/29 and to stage 31 chick (*8*) and stage-equivalent duck embryos, as indicated. In each case, wing and leg buds were removed from the embryos after completion of the whole mount procedure and photographed from a dorsal view.